Heliyon 9 (2023) e20742

Contents lists available at ScienceDirect

Heliyon

journal homepage: www.cell.com/heliyon

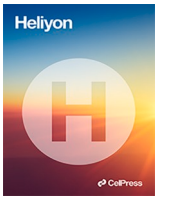

HPLC-UV evaluation of a microwave assisted method as an active drug loading technique for exosome-based drug delivery system

Luisa Fernanda Briones-Márquez [a], José Navarro-Partida [b], Azucena Herrera-González [a], Miguel A. García-Bon [b], Iliany Annel Martínez-Álvarez [c], David Uribe-Rodríguez [c], Luis J. González-Ortiz [a], Edgar J. López-Naranjo [a,*]

[a] CUCEI-Universidad de Guadalajara, 44430, Guadalajara, Jal, Mexico
[b] Tecnológico de Monterrey, Escuela de Medicina y Ciencias de la Salud, Monterrey, 64849, Mexico
[c] Centro de biotecnología SANTER S.C., 45040, Guadalajara, Jal, Mexico

A B S T R A C T

This paper evaluates the potential of a microwave radiation (MR) assisted method as an active drug loading technique for exosomes using polyphenolic nutraceuticals as model drugs (i.e. resveratrol (RV), rosmarinic acid (RA), pterostilbene (PT) and epigallocatechin gallate (EG)). MR is evaluated as a single step method and as part of a two-step method consisting of incubation (IN) followed by MR. The effect of exposure time, loading method and type of nutraceutical on the loading efficiency were investigated using high performance liquid chromatography (HPLC), X-ray diffraction (XRD) and flow cytometry. Additionally, dynamic light scattering (DLS) was used to determine the size of exosomes. Loading efficiency results indicated that MR is a promising method to be used as loading process. Results also suggested that due to different levels of hydrophobicity, related to the number of OH groups, the absorption of polyphenols into the bilayer of EVs is different for each molecule. According to XRD results, MR could not be used with any cargo drug since radiation could affect the chemical composition and the degree of crystallinity of such molecules, consequently affecting their performance. Flow cytometry results indicated that loading methods negatively affect exosome concentration.

1. Introduction

Exosomes are natural nanometric (usually 30–150 nm), specialized extracellular vesicles (EVs) that bear numerous biological molecules including nucleic acids, proteins and lipids that play important roles in intracellular communication (Fig. 1). Exosomes can be obtained from a wide variety of cells and show outstanding stability, appropriate cargo and delivery properties as well as a convenient safety profile. Exosomes-based drug delivery systems offer several advantages over conventional systems including better biocompatibility, lower immunogenicity, and direct drug delivery to cells. Exosomes exhibit increased stability in the bloodstream that allows them to travel long distances within the body under both physiological and pathological conditions. Additionally, due to their hydrophilic core, exosomes are able to encapsulate both hydrophilic and hydrophobic drugs. Since exosomes are nanosized, they are able to successfully cross-different types of biological barriers (e.g. blood-brain, stromal, blood-retinal and placental barriers), which constitute main obstacles that continue to challenge drug delivery systems [1–4]. Furthermore, the immunogenicity of exosomes is very low compared to liposomes and virus-based drug delivery systems [5]. Consequently, exosomes are considered to show great potential to be used as drug delivery vehicles. So far, several passive and active post-isolation methods have been used for exosome-loading with small molecules, proteins and nucleic acids showing different efficiency levels as exemplified in Table 1 [6].

* Corresponding author.
E-mail address: edgar.lopezn@academicos.udg.mx (E.J. López-Naranjo).

https://doi.org/10.1016/j.heliyon.2023.e20742
Received 8 June 2023; Received in revised form 10 September 2023; Accepted 5 October 2023
Available online 6 October 2023

Passive loading (i.e. incubation) does not require the use of active substances or processes, in this procedure drug diffuses into the exosomes due to a concentration gradient. On the other hand, active loading methods, which include mechanical extrusion, saponin permeabilization, transfection, electroporation, direct mixing, freeze-thaw cycles, thermal shock, stirring, sonication and eddy current oscillation and as well as their combinations are based on the application of an external stimulus (e.g. electrical field, mechanical shear force, etc.) These processes are known to slightly disrupt the cell membrane in different ways; inducing temporary formation of pores, breaking down the structure of cells into free lipid and protein molecules or increasing the permeability on exosomal membranes, and consequently allowing cargo entry. However, none of these methods have shown so far optimal results, so new possibilities need to be explored [3,14].

Microwave radiation (MR) is a type of non-ionizing electromagnetic field with a frequency within the range of 300 MHz to 300 GHz that show both thermal and non-thermal effects that is able to increase cell permeability. From 300 MHz to 3 GHz is considered ultra-high frequency, 3–30 GHz MR corresponds to super high frequency and from 30 to 300 GHz corresponds to extremely high frequency radiation. Additionally, MR that exceed a peak power of 100 MW with an operation frequency between 1 and 300 GHz is considered high-power radiation.

MR exists in our daily life environment due to its use in applications such as conventional microwave ovens (~2.45 GHz), radar, navigation systems and spectroscopy. Although, all biological systems could be affected by MR, possible alterations depend upon operating frequencies and peak power. Regarding MR effects on cells, it has been reported that morphology alterations, division disruptions and membrane permeability changes may occur when external fields are sufficiently strong and significantly higher than the voltages generated by mitochondrial membranes. In such case, degeneration, apoptosis or necrosis in cells can occur at different stages depending on the field strength, wave form, modulation and duration of exposure [15–17].

Regarding MR frequency, Verma et al. [18] showed that rat skin exposed to 10 GHz at a power density of 10 mW/cm^2 MR during 3 h/day for 30 days exhibited significant biophysical, biochemical, molecular and histological alterations. MR also led to oxidative stress, inflammatory responses and metabolic alterations. In a similar way, Franchini et al. [19] demonstrated that human fibroblasts exposed to 25 GHz MR at 20 mW did not show apoptosis or alterations in pro-survival signaling proteins; however, MR induced an increased number of micronuclei and centromere-positive micronuclei owing to chromosome loss. Narayanan et al. [20] reported that exposure to 900 MHz, 146.60 mW/cm^2 MR 1 h/day for 28 days resulted in oxidative stress in brain. Deshmukh et al. [21] showed that 900 MHz MR for 2 h a day, 5 days a week for 90 days might lead to a decline in cognitive function on rat brain. Calabrò et al. [22] investigated SH-SY5Y human neuroblastoma cells exposed to MR for 2 and 4 h at 1800 MHz, their results indicated that MR induced a time-dependent decrease in cell viability. However, they also reported that even at these experimental conditions, heat shock gene expression was not affected. In a similar way, Yao et al. [23] showed that mRNA levels of rabbit lens epithelial cells exposed to continuous MR at a frequency of 2450 MHz for 8 h remained unchanged. Koyama et al. [24] reported that human corneal epithelial and human lens epithelial cells exposed to 60 Hz-MR during 24 h had no significant effects on the micronucleus formation frequency or

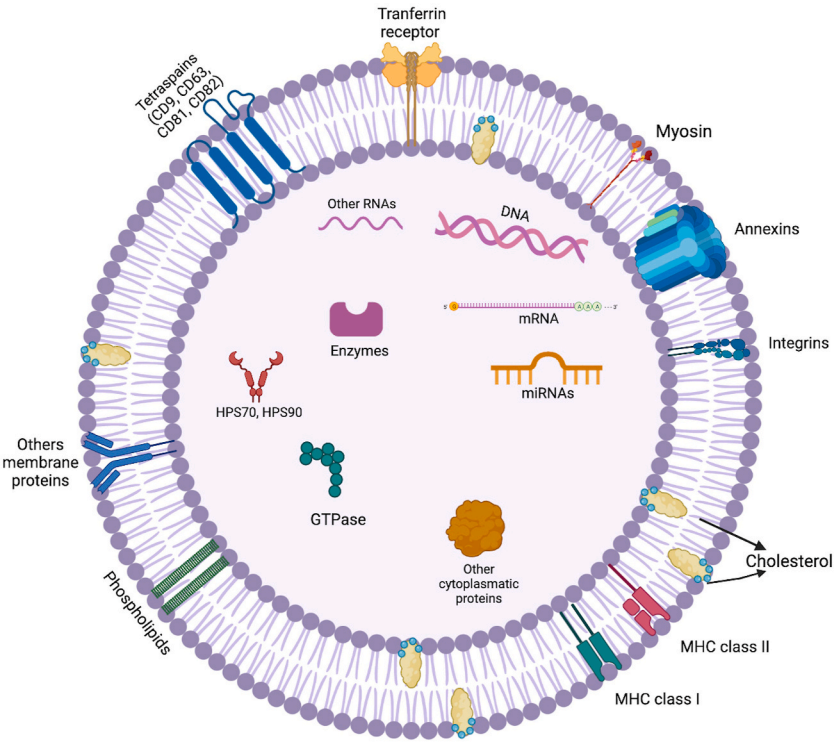

Fig. 1. Representation of exosome structure.

Table 1
Exosome-loading methods and their corresponding efficiencies.

Loading method	Exosome source	Delivery cargo	Efficiency	Reference
Incubation	Prostate cancer cells	Paclitaxel	10.03 %	Saari et al., 2015 [7]
Incubation (for hydrophobic porphyrin) Electroporation (for hydrophilic porphyrin)	a. Breast cancer cells b. Human umbilical vein endothelial cells c. Bone-marrow derived human mesenchymal cells d. Human embryonic stem cells	Porphyrin	Using hydrophobic porphyrin: a. 28.1 (±9.4 %) b. 31.9 (±14.5 %) c. 31.5 (±8.1 %) d. 35.2 (±8.4 %) Using hydrophilic porphyrin: a. 2.9 (±0.5 %) b. 0.6 (±0.2 %) c. 1.6 (±0.7 %) d. 0.8 (±0.4 %)	Furhmann et al., 2015 [8]
Electroporation	Ovarian cancer tumors of SKOV3 xenograft mice	CRISPR/Cas9	~1.75 %	Kim et al., 2017 [9]
Co-incubation (Mixing/ Incubation)	Bovine milk	Paclitaxel	7.9 (±1 %)	Agrawal et al., 2017 [10]
a. Electroporation b. Sonication c. Co-incubation	Raw 264.7 macrophages (mice)	Paclitaxel	a. 5.3 % b. 28.29 % c. 1.44 %	Kim et al., 2016 [11]
Sonication	Pancreatic cancer cells	Gemcitabine	11.68 (±3.68 %)	Li et al., 2020 [12]
Freeze and thaw cycles Incubation	Raw 264.7 macrophages (mouse)	Catalase	14.7 (±1.1 %) 4.9 (±0.5 %)	Haney et al., 2015
Ultracentrifugation	Raw 264.7 macrophages (mouse)	Brain derived neurotrophic factor	~20 %	Yuan et al., 2017 [13]

genotoxicity of such cells. Therefore, it is possible to say that MR does not affect all types of cells in the same way even under similar experimental conditions.

It also seems that duration of exposure is a major determinant of MR effect on living cells, at short times of exposure even at high frequencies no negative effects have been observed. For example, Mishra et al. reported that membrane nucleotides and enzymes of *S. aureus* cells exposed to 24 GHz radiation during 10–40 s remained unaffected [16].

Regarding temperature, it has also been reported that temperature ranging between 40 and 42 °C is not lethal to cells but can lead to alterations in morphology such as cell flattening or membrane ruffling depending on the exposure time. For example, mild thermal stress (40-42 °C for 10–30 min) increases growth and metabolic rates by 20 % and mammalian cells exposed to temperatures ranging 42-46 °C for 30–50 min exhibited dramatically altered morphology and inhibited cell cycle progression and activation of molecular defense mechanisms [25].

On the other hand, nutraceuticals are considered a promising therapeutic approach in ophthalmology. Nutraceuticals can be defined as supplements originated from food that contain a bioactive agent in a greater concentration than in a balanced diet or in a concentration equivalent to it that function as an enhancement for pharmacological treatment, or for the delay, improvement or even prevention of diseases [26].

Therefore, in the present work a microwave assisted method as an active loading technique for exosomes was evaluated and compared to a widely used passive loading method (i.e. incubation) using HPLC-UV to quantify loading efficiency. A 2.45 GHz MR was used as external stimulus at short times (5, 10 s) and at temperatures <40 °C to promote exosome loading. Four different polyphenolic nutraceuticals [i.e. resveratrol (RV), rosmarinic acid (RA), pterostilbene (PT) and epigallocatechin gallate (EG)] were used as model drugs.

2. Materials and methods

2.1. Materials

Resveratrol (>99 %) (RV), rosmarinic acid (>96 %) (RA), pterostilbene (>97 %) (PT) and epigallocatechin gallate (>95 %) (EG), acetonitrile HPLC grade, methanol HPLC grade, methanol (ACS reagent 99.8 %), ethanol (99.8 %, molecular biology), formic acid (ACS reagent 96 %), acetic acid (glacial reagent plus >99 %) and sodium acetate were purchased from Sigma-aldrich. Balanced salt solution (BSS) from Bausch and Lomb was used. Exosomes suspension (78 exosomes/μl) isolated from human umbilical cord – mesenchymal cells (hUC-MSC) were provided by Centro de Biotecnología SANTER and were storage −20 °C until use.

2.2. Sample preparation

RV, RA, PT and EG samples were prepared as follows: 3 mg of each of the aforementioned nutraceuticals were dissolved using 10 ml of solvent. In the case of RV, RA and PT, ethanol was used as solvent while in the case of EG a methanol 50%-distilled water 50 % mixture was employed. 200 μl of each nutraceutical solution was placed separately in an Eppendorf tube to which 200 μl of exosome suspension (containing ~15600 exosomes) were added.

2.3. Drug loading

MR, incubation (IN), and a two-step method consisting of IN followed by MR (IN/MR) were evaluated in this work. To carry out each one of the previously mentioned methods two different devices were used: (1) a conventional microwave oven (Sharp Model No. R-309YW Serial No.D1Y0012192) power input 120 V, operating at a 2.45 GHz frequency. (2) an incubator device Luzeren model DHP-9032 power input 110 V/60 Hz, 200 W. Samples were exposed to MR, IN or IN/MR according to Table 2.

2.4. Dynamic light scattering (DLS)

DLS measurements were carried on in a Malvern Zetasizer 5000 instrument equipped with a 7132 multibit correlator and multiangle goniometer (Malver Panalytical, Malvern UK). The light source employed was a He–Ne laser having a wavelength of 632.8 nm. 3 measurements were performed to determine the size of the exosomes used in the present work. Exosomes average size was found to be 78.70 nm (±36.95).

2.5. High performance liquid chromatography (HPLC)

To analyze the presence of the selected nutraceuticals after loading, and provide quantitative results, HPLC analysis was performed using an Agilent Technologies 1260 device model Infinity equipped with a UV detector, using a C18 column (Phenomenex Luna 5u, 4.6 × 150 mm, 10 nm). Standard stock solutions (SSS) for each nutraceutical were prepared by dissolving each analyte in the corresponding solvent (i.e. ethanol for RV, RA and PT, and methanol 50 %/distilled water 50 % mixture for EG). SSS were diluted to prepare working standard solutions to generate the corresponding calibration curves with at least five different concentration levels each. Samples for analysis were prepared by taking 100 μl of each supernatant media collected after samples were exposed to the experimental conditions described in Table 2. Chromatographic analysis was performed according to the experimental conditions indicated in Table 3 for each selected nutraceutical [27–31]. Loading efficiency was evaluated using an indirect method, calculating the amount of unincorporated drug by means of HPLC analysis. In that way, loading efficiency was estimated subtracting the free drug content in the supernatant after centrifugation from total drug content [3]. Statistical analysis of loading efficiencies is presented as the mean value of three different assays and their corresponding SD for each one of the 11 experimental conditions described in Table 2, analyzing the effect of the loading method (i.e IN, MR, IN/MR) and the exposure time separately.

2.6. X-ray diffraction (XRD) tests

A Panalytical Empyream device with a copper anode as X-ray source (Cu, $\lambda = 0.154059$ nm operating at 40 kV and 30 mA) was used. Difractograms were analyzed from the initial angle $2\theta = 5^{\circ}$ to the final angle 50°, with scanning rate 5°/min and step size of 0.02 to determine the crystallographic structure and analyze structural changes in all selected nutraceuticals due to their exposure to the different loading methods evaluated in this work. Solid samples of each nutraceutical were placed on a zero-background silicon sample holder for improved signal quality.

2.7. Flow cytometry

Flow cytometry was performed employing a MACSPlex kit and a MACSQuant Miltenyi-Biotec analyzer to quantify the number of

Table 2
Loading efficiencies (%) for selected nutraceuticals.

Condition	Drug loading method	Exposure time	Loading efficiency % (SD)			
			RV	RA	PT	EG
1	IN	10 min	81.79 (0.19)	70.92 (0.24)	99.81 (0.01)	47.48 (0.61)[a]
2	IN	30 min	87.06 (0.19)	73.83 (0.30)	99.83 (0.01)	49.81 (1.64)
3	IN	60 min	88.58 (0.04)	74.36 (0.26)	99.84 (0.01)	50.76 (0.55)
4	MR	5 s	81.26 (0.26)	76.61 (0.32)	99.97 (0.01)[a]	50.69 (0.54)
5	MR	10 s	77.13 (0.17)[a]	76.92 (0.30)	99.96 (0.01)	58.41 (0.51)[a]
6	IN/MR	10 min/5 s	87.17 (0.18)	76.97 (0.43)	99.96 (0.01)[a]	53.09 (0.48)
7	IN/MR	10 min/10 s	92.65 (0.02)[a]	73.08 (0.37)	99.81 (0.01)	52.24 (0.50)
8	IN/MR	30 min/5s	82.25 (0.30)	76.91 (0.27)	99.8 (0.01)	57.67 (0.18)[a]
9	IN/MR	30 min/10 s	83.95 (0.05)	68.34 (0.42)[a]	99.72 (0.01)[a]	54.57 (0.32)
10	IN/MR	60 min/5 s	93.49 (0.16)[a]	77.44 (0.25)[a]	99.75 (0.02)	56.89 (1.04)
11	IN/MR	60 min/10 s	75.63 (0.30)[a]	77.55 (0.46)[a]	99.85 (0.01)	53.20 (0.72)

[a] Samples were incubated at 25 °C. In the case of samples exposed to MR, temperatures of 28.3 and 37.9 °C were registered for 5 and 10 s of MR exposure respectively. Loading efficiency is presented as the mean of percentage ± standard deviation (SD) from three different assays. For the contrast of drug loading methods with different exposure times, the Kruskal-Wallis H test was used. Dunn's test was performed for pairwise comparisons. A statistically significant p value (<0.05) is emphasized by an asterisk. RV: Resveratrol, RA; Rosmarinic acid, PT: Pterostilbene, EG: Epigallocatechin gallate, IN: Incubation, MR: Microwave radiation, SD: Standard deviation.

Table 3
Chromatographic conditions.

Nutraceutical	Wavelength (nm)	Column	Mobile phase	Flow rate (ml/min)	Injection volume (μl)	Run time (min)	Method
RV	310	C18 150 × 4.6 mm, i.d. 5 μ	A: 1 % (v/v) acetic acid in distilled water B: Methanol	0.8	5	17	17 min gradient schedule: (a) 0–5 min: A60 %:B40 % (b) 5–10 min: A35 %:B65 % (c) 10–15 min: A10 %:B90 % (d) 15–17min: A60 %:B40 %
RA	362	C18 150 × 4.6 mm, i.d. 5 μ	A: Distilled water acidified with formic acid (pH = 2.5) B: ACN	0.8	20	20	Isocratic mode
PT	320	C18 150 × 4.6 mm, i.d. 5 μ	A: 0.1 % (v/v) formic acid B: ACN	0.8	25	10	10 min gradient schedule: (a) 0–4 min: ACN 60 % (b) 4–7 min: ACN 60–90 % (c) 7–10 min: ACN 90 %
EG	303	C18 150 × 4.6 mm, i.d. 5 μ	A: AcB (1.0 mM acetic acid, 1.0 mM sodium acetate (pH = 4.5) B: ACN	0.7	20	15	17 min gradient schedule: (a) 0–9 min: A88 %:B12 % (b) 9–14 min: A79 %:B21 % (c) 14–17 min: A40 %:B60 %

ACN: Acetonitrile, AcB: Acetate buffer.

exosomes per μl of sample using 37 distinct exosome markers and 2 controls. Sample preparation: Separately, 120 μl of PBS buffer (used as control sample), 120 μl of cell culture supernatant and 120 μl of each experimental sample were placed in 1.5 ml microfuge tubes. 15 μl of magnetic exosome capture beads were added to each tube, which were gentle vortexed to resuspend samples completely. MACSPlex detection reagent was added to each tube. Tubes were incubated during 1 h under continuous stirring and protected from sunlight. Subsequently, 500 μl of MACSPlex buffer were added to each tube, which were centrifuged at 3000×*g* during 5 min. 500 μl of supernatant were then carefully aspired. Finally, 500 μl of MACSPlex buffer were added before exosome quantification.

2.8. Statistical analysis

Quantitative variables were described using mean and standard deviation. Qualitative variables were described using frequencies and percentages. Loading efficiency is presented as the mean of percentage ± standard deviation (SD) from three different assays. For the contrast of drug loading methods with different exposure times, the Kruskal-Wallis H test was used. Dunn's test was performed for pairwise comparisons between groups. A statistically significant p value was defined as $p < 0.05$. The statistical analyses were done using the SPSS 22.0 software (SPSS, Inc., Chicago, IL, USA) and graphs were made with GraphPad Prism 9.0.0 (San Diego, California USA).

3. Results and discussion

3.1. HPLC

Chromatographic results indicate that the loading efficiency is modified by both, the method and the exposure time. Remarkably, the combination of IN and MR (IN/MR conditions) significantly increased the drug loading in exosomes in all cases. Comparisons of the mean percentage of loading efficiency are presented in Fig. 2. It can also be observed that for RV and RA IN/MR 60 min/5s produced the best loading results, while IN/MR 30 min/10 s was the best method when PT was used and IN/MR 30 min/5 s in the case of EG as model drug.

Regarding the type of nutraceutical evaluated, it is clear that PT showed the best loading results regardless of the loading method analyzed, followed by RV, RA, and EG (i.e. loading efficiency: PT > RV > RA > EG), which is related to the hydrophobic nature of the polyphenolic nutraceuticals evaluated in this work. Polyphenols can variably interact with and penetrate lipid bilayers depending on their structure, as the number of OH groups increases, the hydrophobicity of the compound decreases, negatively affecting their absorption. Thus, PT which shows the lowest number of OH groups showed the highest loading efficiencies while EG which contains the highest number of OH groups showed the lowest loading efficiencies [32].

3.2. XRD

XRD was carried out to analyze the changes in the composition and the crystalline nature of the nutraceuticals due to their exposure

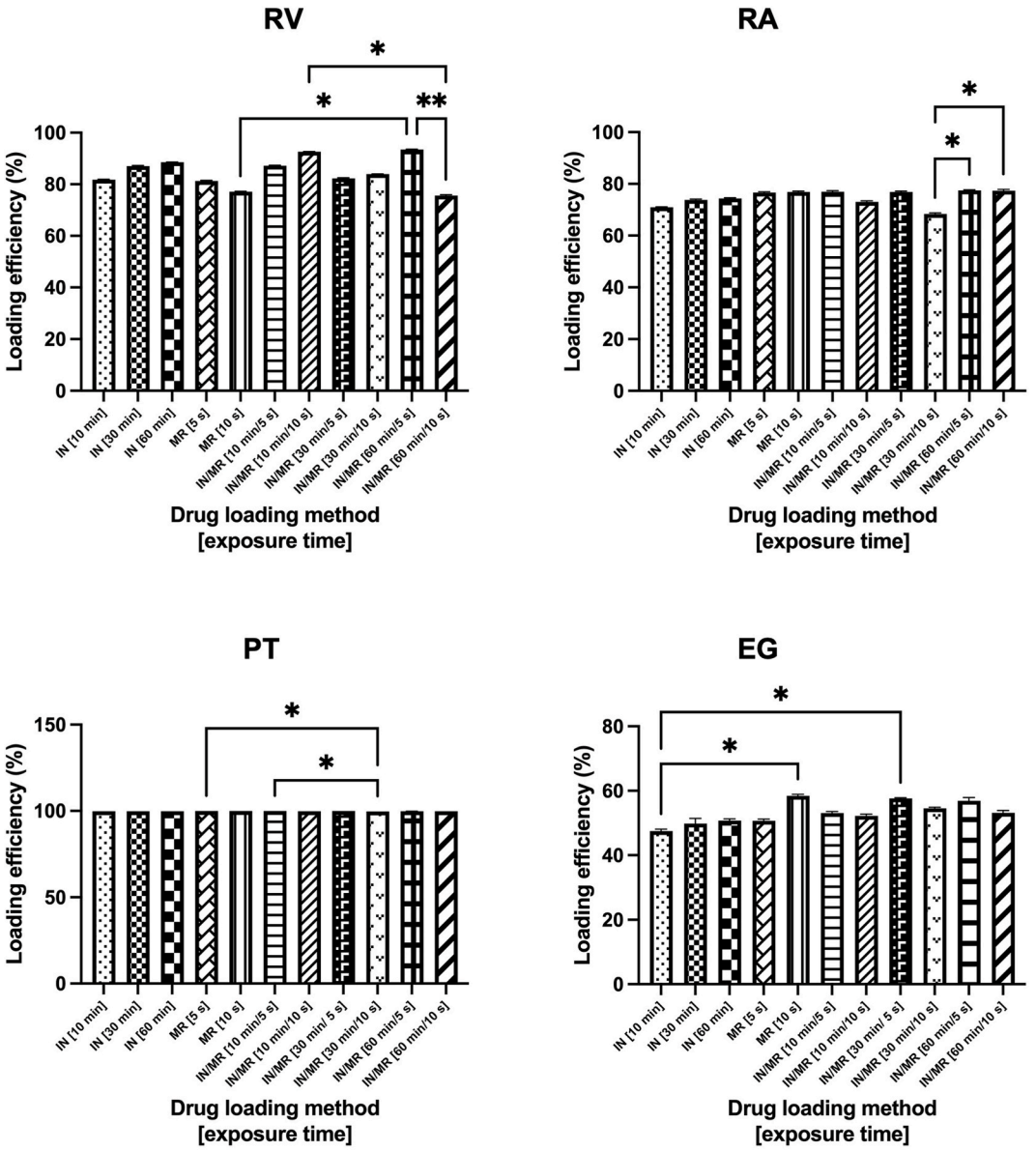

Fig. 2. Effect of the drug loading method in the exosomes drug loading efficiencies for selected nutraceuticals. IN and MR exosomes drug loading methods with different exposure times were analyzed for RV, RA, PT and EG. We observed that the combination of IN and MR (IN/MR conditions) significantly increases the drug loading in exosomes in all cases. Pairwise comparisons with P value less than 0.05 are displayed with asterisks and lines (*; P value less than 0.05, **; P value less than 0.01). Samples were incubated at 25 °C. In the case of samples exposed to MR, temperatures of 28.3 and 37.9 °C were registered for 5 and 10 s of MR exposure respectively. EG; Epigallocatechin gallate IN; Incubation, MR; Microwave radiation, PT; Pterostilbene, RA; Rosmarinic acid, RV; Resveratrol, SD; standard deviation.

to IN and MR. Samples exposed to IN-60 min and MR-10 s, which correspond to experimental conditions 3 and 5 respectively for each nutraceutical (i.e. maximum exposure time to each process) were analyzed to evaluate the effect of both loading processes on RV, RA, PT and EG. XRD results are shown in Fig. 3. Regarding RV, according to Sun et al. [33] XRD pattern of pure RV shows intense characteristic peaks at 2θ diffraction angles of 6.6 16.4, 19.1, 22.3, 28.3°, as well as some other weak intensity peaks, which confirm the crystalline nature of RV. Fig. 3a (RV-3) and 3b (RV-5) show all the characteristic peaks corresponding to RV, indicating that the chemical compositions of samples exposed to IN and MR are identical to that of pure RV. Regarding RA, XRD patterns were previously identified by Huang et al. [34] and correspond to peaks at diffraction angles of 12.97, 13.92, 15.40, 19.73, 24.19, 27.03, 29.46°. In a similar way to RV, the characteristics peaks of RA can be clearly observed in Fig. 3c (RA-3) and 3d (RA-5), indicating that no changes in the composition took place. For EG, the characteristic crystalline peaks appear at 8.50, 10.36, 15,63, 17.06, 20.75, 21.51, 24.52, 25.90, 28.95 and 35.53° [35]. In this case, it seems that IN (Fig. 3e) had no negative effects on the chemical composition or the degree of

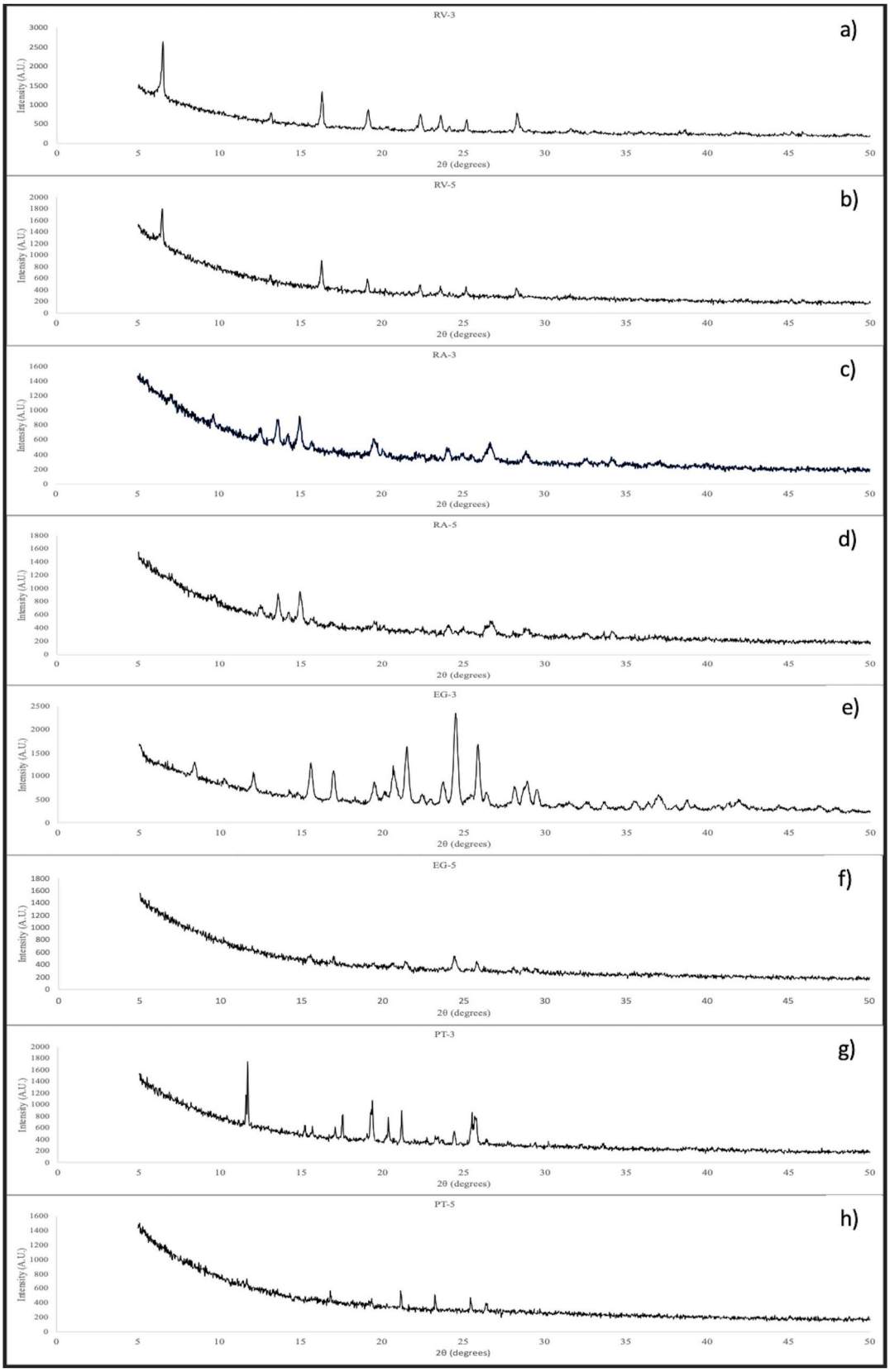

(caption on next page)

Fig. 3. XRD patterns of nutraceuticals exposed to loading methods: a) RV-3 (RV – IN 60 min), b) RV-5 (RV – MR 10 s), c) RA-3 (RA – IN 60 min), d) RA-5 (RA – MR 10 s), e) EG-3 (EG – IN 60 min), f) EG-5 (EG – MR 10 s, g) PT-3 (PT – IN 60 min), h) PT-5 (PT – MR 10 s). EG; Epigallocatechin gallate IN; Incubation, MR; Microwave radiation, PT; Pterostilbene, RA; Rosmarinic acid, RV; Resveratrol.

crystallinity of the nutraceutical. However, it is clear that MR (Fig. 3f) degraded EG since its XRD pattern and the intensity of the peaks are completely different from those reported for pure EG. Therefore, the chemical composition and degree of crystallinity of EG was completely modified due to its exposure to EG. Finally, in the case of PT, XRD pattern include peaks at 12, 15.3, 16.7, 18, 20.2, 20.7, 23 and 25.4° [36]. Main peaks can be identified in both difractograms, PT-3 (Fig. 3g) and PT-5 (Fig. 3h), which means that the chemical composition did not change. However, the intensity of the diffraction peaks is different among them, indicating differences in the degree of crystallinity. According to these results, MR produced a decrease in the degree of crystallinity of PT, increasing its amorphous

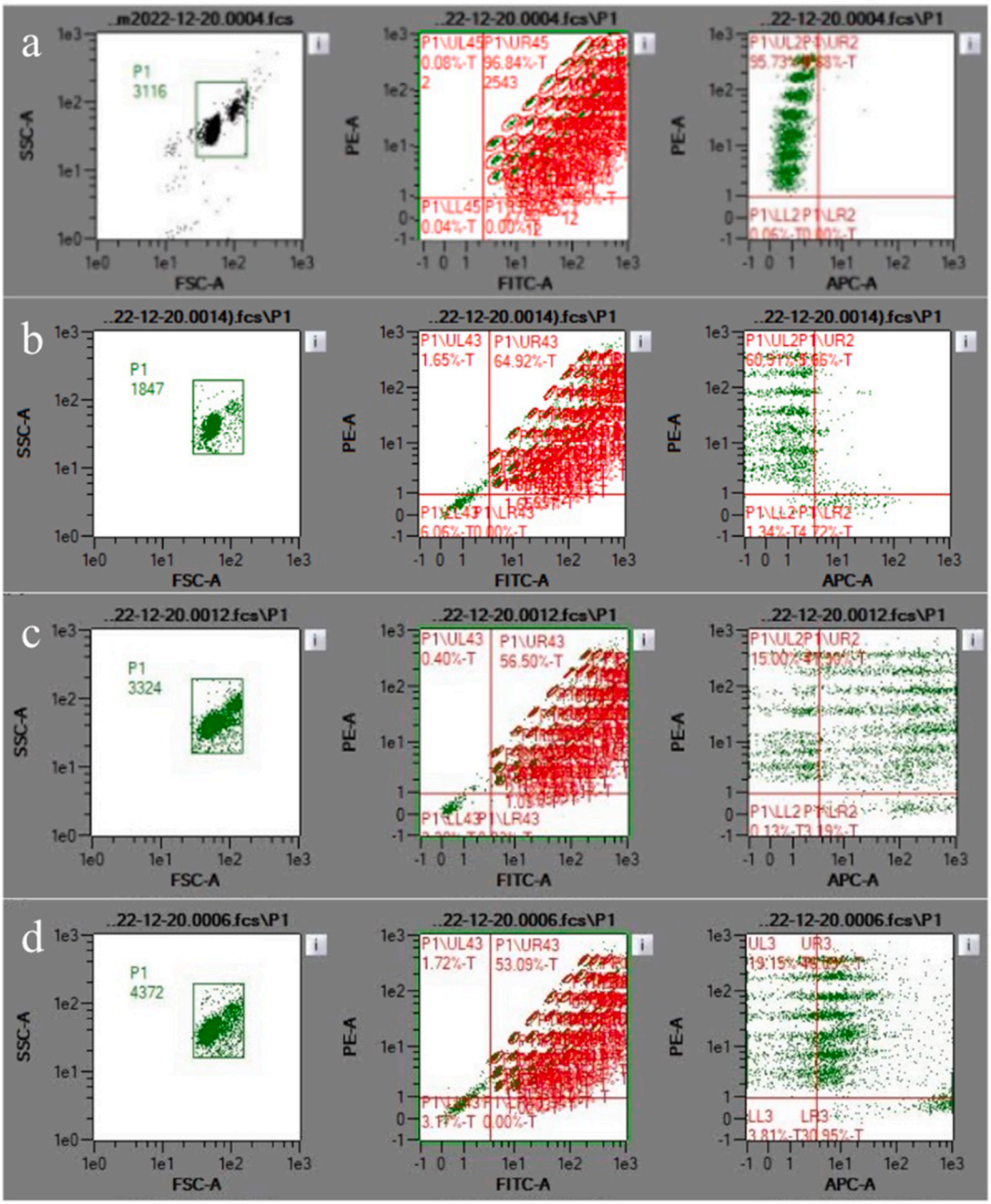

Fig. 4. Flow cytometry results: a) Calibration beads, b) PBS buffer (used as reference), c) Exosome non-exposed to loading processes, d) Exosomes exposed to MR – 10 s. PBS: Phosphate buffer saline.

phase [37,38]. Therefore, the integrity of some cargo drugs (in this case nutraceuticals) could be compromised due to its exposure to MR either independently or in combination with another loading process (e.g. IN) depending on their nature.

3.3. Flow cytometry

Flow cytometry was performed for non-loaded exosome suspension (i.e. non-exposed to IN or MR) and exosome suspensions exposed to experimental conditions (3, 5 and 11), that is exposed to IN 60 min, MR 10 s and IN/MR 60min/10s respectively to analyze the effect of IN and MR on exosomes. The concentration of exosomes in the suspensions non-exposed to any loading method was 78 exosomes/μl (i.e. initial concentration). According to flow cytometry results, after IN 60 min exosomes concentration was reduced to 28 exosomes/μl. In the case of exosomes exposed to MR 10s, a concentration of 56 exosomes/μl was found. Finally, in the case of exosomes exposed to IN/MR 60 min/10s a concentration of 19 exosomes/μl was registered. Therefore, it seems that IN has a more deleterious effect on exosomes since the presence of this EVs decreased to a greater extent than in the case of samples exposed to MR. Evidently, in the case of the two-step process (IN/MR) the decrease was even greater. Fig. 4. Exemplifies Flow cytometry results. Fig. 4a corresponds to calibration beads. It can be observed the following information: (left): Gate selection by size and granularity, (center): 37 Markers 2 and controls labeled by pearls and antibodies, (right): regions labeled by calibration beads (upper left quadrant) as autofluorescence control, giving a negative result to exosome adherence (right left quadrant). In a similar way to Fig. 4a, in Fig. 4b which corresponds to PBS buffer (used as reference), the following information can be observed: (left): Gate selection by size and granularity, (center): 37 Markers 2 and controls labeled by pearls and antibodies, (right): regions labeled by calibration beads (upper left quadrant) giving a negative result to exosome adherence (right left quadrant). On the other hand, Fig. 4c, which corresponds to non-loaded exosomes shows (left): Gate selection by size and granularity, (center): 37 Markers 2 and controls labeled by pearls and antibodies, (right): regions labeled by calibration beads (upper left quadrant) giving a positive result to exosome adherence (right left quadrant), 78 exosomes/μl were quantified. Finally, in Fig. 4d corresponding to exosomes exposed to MR – 10 s, (left): Gate selection by size and granularity, (center): 37 Markers 2 and controls labeled by pearls and antibodies, (right): regions labeled by calibration beads (upper left quadrant) giving a positive result to exosome adherence (right left quadrant), 56 exosomes/μl were quantified.

4. Conclusions

The potential of MR as an active loading method has been evaluated. Statistical analysis of loading efficiencies obtained from exosomes loaded with different nutraceuticals under a wide variety of experimental conditions indicated that a combined process consisting of incubation followed by exposure to microwave radiation (IN/MR) significantly increased drug loading in all cases. Regarding each loading process independently, results indicate that microwave radiation is a promising candidate to be used as loading method since similar loading efficiencies to those of exosomes exposed to incubation were obtained. XRD results indicated that not any drug could be loaded into exosomes using microwave radiation since degradation of the cargo drug could take place. Changes in the chemical composition and/or the degree of crystallinity could take place and consequently affect the performance of particular drugs. In addition, flow cytometry results showed that incubation decreased exosomes concentration to a greater extent than microwave radiation, this may be due to longer exposure periods, which are necessary when incubation is used as a loading method.

Data availability

Data will be available on request (contact information: Edgar López, edgar.lopezn@academicos.udg.mx).

Declaration of competing interest

The authors declare that they have no known competing financial interests or personal relationships that could have appeared to influence the work reported in this paper.

Acknowledgements

This work was supported by the Centro Universitario de Ciencias Exactas e Ingenierías, Universidad de Guadalajara.

References

[1] M. Xu, et al., Recent advancements in the loading and modification of therapeutic exosomes, Front. Bioeng. Biotechnol. 8 (2020) 1–12.
[2] R.O. Elliott, M. He, Unlocking the power of exoosmes for crossing biological barriers in drug delivery, Pharmaceutics 13 (122) (2021) 1–20.
[3] J. Wang, D. Chen, E.A. Ho, Challenges in the development nad establishment of exosome-based drug deliver systems, J. Contr. Release 10 (329) (2020) 894–906.
[4] H. Chen, et al., Exosomes, a new star for targeted delivery, Front. Cell Dev. Biol. 9 (2021) 1–20.
[5] X.C. Jiang, J.Q. Gao, Exosomes as novel bio-carriers for gene and drug delivery, Int. J. Pharm. 521 (2017) 167–175.
[6] H. Zeng, et al., Current strategies for exosome cargo loading and targeting delivery, Cells 12 (1416) (2023) 1–23.
[7] H. Saari, et al., Microvesicle-and exosome mediated drug delivery enhances the citotoxicity of paclitaxel in autologous protate cancer cells, J. Contr. Release 220 (2015) 727–737.
[8] G. Fuhrmann, et al., Active loading into extracellular vesicles significantly improves the cellular uptake and photodynamic effect of porphyrins, J. Contr. Release 205 (2015) 35–44.

[9] S.M. Kim, et al., Cancer-derived exosomes as a delivery platform of CRISPR/Cas9 confer cancer cell tropism-dependent targeting, J. Contr. Release 266 (2017) 8–16.
[10] A.K. Agrawal, et al., Milk-derived exosomes for oral delivey of paclitaxel, Nanomedicine: NBM (NMR Biomed.) 13 (5) (2017) 1627–1636.
[11] M.J. Haney, et al., Exosomes as drug delivery vehicles for Parkinson's disease therapy, J. Contr. Release 207 (2015) 18–30.
[12] Y.J. Li, et al., Gemcitabine loaded autologous exosomes for effective and safe chemotherapy of pancreatic cancer, Acta Biomater. 101 (2020) 519–530.
[13] D. Yuan, et al., Macrophage exosomes as natural nanocarriers for protein delivery to inflamed brain, Biomaterials 142 (2017) 1–12.
[14] M.N. Oskouie, et al., Therapeutic use of curcumin-encapsulated and curcumin-primed exosomes, J. Cell. Physiol. 234 (6) (2019) 8182–8191.
[15] X. Zhao, G. Dong, C. Wang, The non-thermal biological effects and mechanisms of microwave exposure, Int J Radiat Res 19 (3) (2021) 483–494.
[16] T. Mishra, et al., Effect of low power microwave radiation on microorganism and other life forms, Adv Microw Wirel Technol 1 (1) (2013) 4–11.
[17] S. Mumtaz, et al., Microwave radiation and the brain: mechanisms, current status, and future prospects, Int. J. Mol. Sci. 23 (9288) (2022) 1–26.
[18] S. Verma, et al., Effects of microwave 10 GHz radiation exposure in the skin of rats: an insight on molecular responses, Radiat. Res. 196 (4) (2021) 404–416.
[19] V. Franchini, et al., Genotoxic effects in human fibroblasts exposed to microwave radiation, Health Phys. 115 (1) (2018) 126–139.
[20] S.N. Narayanan, et al., Evaluation of oxidant stress and antioxidant defense in discrete brain regions of rats exposed to 900 MHz radiation, Bratisl. Lek. Listy 115 (5) (2014) 260–266.
[21] P.S. Deshmunkh, et al., Effect of low level subchronic microwave radiation on rat brain, Biomed. Environ. Sci. 29 (12) (2016) 858–867.
[22] E. Calabro, et al., Modulation of heat shock protein response in SH-SY5Y by mobile phone microwaves, World J. Biol. Chem. 3 (2) (2012) 34–40.
[23] K. Yao, et al., Low power microwave radiation inhibits the proliferation of rabbit lens epithelial cells by upregulating P27Kip1 expression, Mol. Vis. 10 (25) (2004) 138–143.
[24] S. Koyama, et al., Effectos of long-term exposure to 60 GHz milimeter-wavelength radiation on the genotoxicity and heat shock protein (HSP) expression of cells derived from human eye, Int. J. Environ. Res. Publ. Health 13 (802) (2016) 1–9.
[25] B. Roy, S. Niture, M.H. Wu, Biological effects of low power nonionizing radiation: a narrative review, J. Radiat. Res. 1 (1) (2021) 1–23.
[26] A. González-Sarrías, et al., Nutraceuticals for older people: facts, fictions and gaps in knowledge, Maturitas 75 (4) (2013) 313–334.
[27] I. Sánchez-Darias, Separación y cuantificación del ácido romarínico en plantas medicinales, in: Química, Universidad de La Laguna: San Cristobal de la Laguna, España, 2018, p. 38.
[28] A.S. Bustos, et al., Cuantificación de resveratrol en vinos mediante HPLC, Rev Boliv Quim 29 (2) (2012) 161–166.
[29] H.S. Lin, B.D. Yue, P.C. Ho, Determination of pterostilbene in rat plasma by a simple HPLc-UV method and its application in preclinical pharmacokinetic study, Biomed. Chromatogr. 23 (12) (2009) 1308–1315.
[30] V. Canelas, C. Teixeira da Costa, Quantitative HPLC analysis of rosmarinic acid in extracts of Melissa officinalis and spectrophotometric measurement of their antioxidant activities, J Chem. Educ. 84 (9) (2007) 1502–1504.
[31] S.T. Saitol, et al., A method for fast determination of epigallocatechin gallate (EGCG), epicatechin (EC), catechin (C) and caffeine (CAF) in green tea using HPLC, Cienc. Tecnol. Aliment. 26 (2) (2006) 394–400.
[32] M. Karonen, Insights into Polyphenol-Lipid interactions: chemical methods, molecular aspects and their effects on membrane structures, Plants 11 (1809) (2022) 1–23.
[33] R. Sun, et al., Lipid based nanocarriers with different lipid compositions for topical delivery of resveratrol: comparative analysis of characteristics and performance, J. Drug Deliv. Sci. Technol. 24 (6) (2014) 591–600.
[34] J. Huang, et al., Investigating the phospholipid effect on the bioaccessibility of rosmarinic acid-phospholipid complex through a dynamc gastrointestinal in vitro model, Pharmaceutics 11 (156) (2019) 1–18.
[35] W. Zhao, et al., Preparation and characterization of epigallocatechin-3-gallate loaded melanin nanocomposite (EGCG@MNPs) for improved thermal stability, antioxidant and antibacterial activity, LWT 154 (112599) (2022) 1–10.
[36] W.S. Tzeng, et al., Pterostilbene nanoparticles downregulate hypoxia-inducible factors in hepatoma cells under hypoxic conditions, Int. J. Nanomed. 16 (2021) 867–978.
[37] S.A.A. Terohid, et al., Effect of growth time on structural, morphological and electrical properties of tungsten oxide nanowire, Appl Phys A 124 (567) (2018) 1–9.
[38] X. Tang, et al., Photoindued degradation of methylammonium lead triiodide perovskite semiconductors, J. Mater. Chem. A 4 (2016) 15896–15903.